

ARMY RESEARCH LABORATORY



High-Obliquity Impact of a Compact Penetrator on a Thin Plate: Penetrator Splitting and Adiabatic Shear

by J. W. Walter
and P. W. Kingman

ARL-TR-1584

January 1998

19980202 041

DMC QUALITY EXPECTED 3

The findings in this report are not to be construed as an official Department of the Army position unless so designated by other authorized documents.

Citation of manufacturer's or trade names does not constitute an official endorsement or approval of the use thereof.

Destroy this report when it is no longer needed. Do not return it to the originator.

Army Research Laboratory

Aberdeen Proving Ground, MD 21005-5066

ARL-TR-1584

January 1998

High-Obliquity Impact of a Compact Penetrator on a Thin Plate: Penetrator Splitting and Adiabatic Shear

J. W. Walter, P. W. Kingman
Weapons and Materials Research Directorate, ARL

DTC QUALITY INSPECTED 3

Abstract

Computational simulations were performed of the impact of a compact, nonideal penetrator on a thin plate at high obliquities. These computations simulated two series of experiments at velocities of 1.5 km/s and 4.1 km/s, respectively, with obliquities of 55–70°.

The experimental results indicated penetrator splitting at obliquities between 55 and 65°. Preliminary three-dimensional simulations with the CTH code, using either maximum tensile stress failure or the Johnson-Cook model, captured some aspects of fragment splitting but in a less than satisfactory manner. Simulations utilizing the Silling shear band model were also performed, with somewhat more realistic results.

In addition to graphical descriptions of the target hole geometry and debris cloud, numerical histories of the target hole area and up-range/down-range partitioning of mass, momentum, and energy were extracted for comparison with the experiments.

Acknowledgment

This work was supported in part by the U.S. Army CORPSAM Project Office.

INTENTIONALLY LEFT BLANK.

Table of Contents

	<u>Page</u>
Acknowledgment	iii
List of Figures	vii
List of Tables	vii
1. Introduction	1
2. Experimental Motivation	1
3. Simulation Methodology	2
4. Results of Simulations	6
5. Discussion	12
6. References	17
Distribution List	19
Report Documentation Page	29

INTENTIONALLY LEFT BLANK.

List of Figures

<u>Figure</u>		<u>Page</u>
1.	Computational Domain for $\theta = 55^\circ$ Showing Symmetry Plane at $y = 0$	3
2.	Combined Effects of Obliquity, θ , and Rotation, ϕ , on Debris Cloud Evolution at 4.1 km/s and 26 μ s; Impact Velocity Vector Lies in x-z Plane	7
3.	Time History of the Penetrator Mass Fraction Exiting the Bottom of the Target at 4.1 km/s	11
4.	Time History of Target Hole Area Normalized by Sphere-Equivalent Penetrator Area at 4.1 km/s.	11
5.	Central Section ($y = 0$) Plots at 1.5 km/s, 60 μ s, and 60° Obliquity Showing Effect of Penetrator Material Failure Model on Fragmentation	13
6.	Behavior of the Two-Dimensional (2D) Explicit Shear Band Model at 1.5 km/s, 24 μ s	14

List of Tables

1.	Summary of Three-Dimensional (3D) Simulations Performed for UAH Shots ...	4
2.	Summary of 3D Simulations Performed for ARL Shots	4

INTENTIONALLY LEFT BLANK.

1. Introduction

A generic problem arising in penetration mechanics is the impact of a compact, nonideal penetrator on a thin plate or shell at high obliquity. We are concerned generally with impacts for which $\theta \geq 55^\circ$, $1.5 \text{ km/s} \leq V \leq 5 \text{ km/s}$, $t/d < 1$, $l/d < 3$, where θ is the obliquity, V the impact speed, t the plate thickness, and l and d the penetrator length and diameter. Ballistic impact under these conditions has been studied relatively little as compared with the large volume of extant work concerned with rigid penetrators and/or low obliquities. Consequently, analytic penetration/debris models and algorithms that are acceptably accurate for encounter conditions of the latter sort may not be so for those considered here. High-obliquity impact on thin targets may produce very asymmetric debris clouds, whereas current penetration algorithms often assume the debris cloud is axisymmetric. Moreover, in thin-target impacts, the relative strength of shear loading as compared with pressure loading increases dramatically at high obliquity so that the operative material failure mechanisms may be quite different from those that apply at the same impact speed but low obliquity.

The work reported herein represents our preliminary effort to include in numerical simulations some of the critical material failure mechanisms which we believe underlie the complex penetration phenomena observed experimentally for encounter conditions described in the previous paragraph. Therefore, we restrict attention to a single prismatic penetrator and single-element target configuration. Geometric variation is primarily with respect to obliquity; we also present results arising from combined effects of penetrator obliquity, θ , and rotation about the shot line, ϕ . Because this study is exploratory, we restrict attention to impact speeds near the extrema of the test matrix.

2. Experimental Motivation

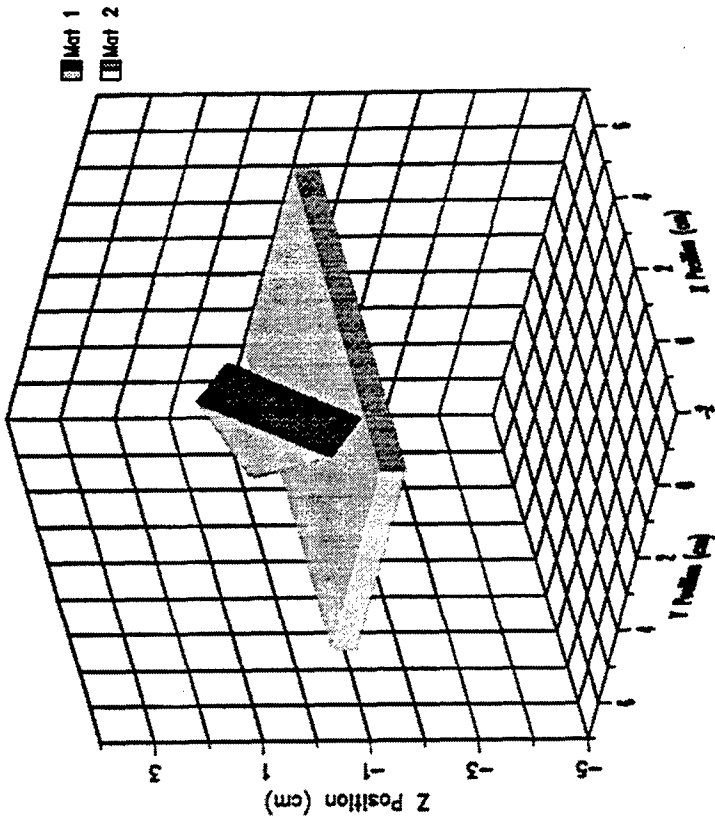
Our simulations were motivated by two series of experiments. The first series was performed at the University of Alabama-Huntsville (UAH) Light Gas Gun for the U.S. Army Missile Command (MICOM); we received a summary of the experiments from Mr. Mike Cole of MICOM. In all shots, the penetrator was a $1.4 \times 2 \times 2$ cm rectangular prism of 4130 steel (density 7.9 g/cm^3 , mass 44.2 g)

hardened to Rockwell C43. The target was a $0.476 \times 150 \times 300$ cm plate of 304 stainless steel. In the experiments, the penetrator orientation (pitch, yaw and θ) varied widely. Rather than attempting to match the geometry of each shot exactly, we performed simulations at each combination of (V, θ) represented in the experiments; at the extreme values of (V, θ) we also varied θ . Figure 1 illustrates the initial geometry used in the simulations. The penetrator faces are parallel and perpendicular to the shot line, and it travels to the right and down. Note that in all the simulations $y = 0$ is exploited as a symmetry plane. Table 1 summarizes the matrix of simulations for the UAH shots.

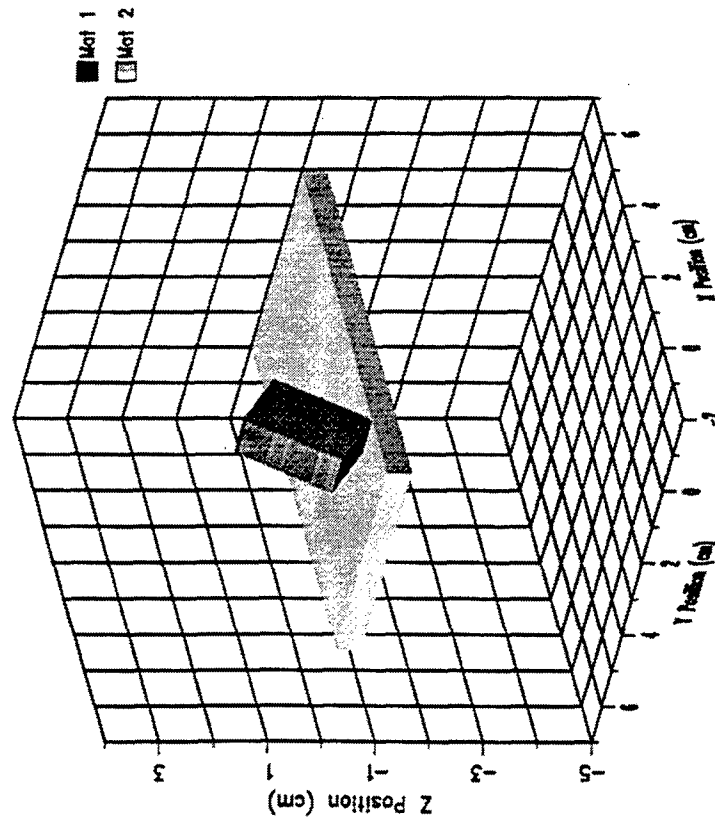
A similar series of experiments were conducted (Bjerke, Luther, and Scheffler 1994) at the U.S. Army Research Laboratory (ARL) (also for MICOM) in which the same penetrator impacted a laminate target at $V \approx 2.2$ km/s and $55^\circ \leq \theta \leq 70^\circ$; yaw and pitch at impact were negligible. The ARL target consisted of a thin, ($t \approx 1.5$ cm), mild steel layer in front, a middle layer of very low-density material, and finally the same stainless plate used in the UAH experiments. For obliquities between 55° and 65° , the penetrator split so that a substantial fragment penetrated the target (and was captured in a witness pack), while other large fragments ricocheted down the front surface of the target. Similar behavior has also been observed for mild steel cube and sphere penetrators against single mild steel and stainless steel plates (Finnegan et al. 1993; Finnegan and Schulz 1992). It appears that this *splitting* mode of penetration is not due primarily to the laminate nature of the ARL target but is dependent upon material strength-related failure mechanisms. In particular, the larger penetrator fragments retained sharp edges and appeared to have suffered little gross plastic deformation. Thus, we chose to examine this phenomenon with simulations at low velocity ($V = 1.5$ km/s, $\phi = 0$) and the same obliquities as in the UAH series. However, we employed several different material models for the penetrator, as noted in Table 2.

3. Simulation Methodology

All simulations were performed with the Eulerian wavecode, CTH (McGlaun and Thompson 1990). The SESAME Mie-Grüneisen EOS model and parameter values for 304 stainless steel were used for the target plate. The deviatoric response was modeled with an elastic-perfectly plastic



(a)



(b)

Figure 1. Computational Domain for $\theta = 55^\circ$ Showing Symmetry Plane at $y = 0$. (a) Shot Line Rotation $\phi = 0^\circ$; (b) Shot Line Rotation $\phi = 45^\circ$. Pitch and Yaw Relative to the Shot Line Are Always Zero.

Table 1. Summary of Three-Dimensional (3D) Simulations Performed for UAH Shots

ID	q	w	g	e	m	k	b	r	c	d	a	v
V (km/s)	4.16	4.16	4.19	4.10	4.16	4.16	3.19	3.19	3.12	3.07	3.11	3.11
θ (deg.)	55	55	60	65	70	70	55	55	60	65	70	70
ϕ (deg.)	0	45	0	0	0	45	0	45	0	0	0	45

Table 2. Summary of 3D Simulations Performed for ARL Shots

ID	θ (deg.)	Penetrator Material Model
x	60	Johnson-Cook flow and failure, $\epsilon^{pf} = 0.6$.
z	60	Johnson-Cook flow and failure, $\epsilon^{pf} = 0.15$.
0	60	Elastic-perfectly plastic, fracture stress = $1.5 Y_0$.
1	60	Elastic-perfectly plastic, fracture stress = $0.375 Y_0$.
3	55	Elastic-perfectly plastic, fracture stress = $1.5 Y_0$.
4	65	Elastic-perfectly plastic, fracture stress = $1.5 Y_0$.
5	70	Elastic-perfectly plastic, fracture stress = $1.5 Y_0$.

(EPP), von Mises yield surface with low-density and high-temperature strength reduction (EPP); the initial yield strength $Y_{02} = 0.34$ GPa was obtained from the Steinberg-Guinan-Lund viscoplasticity model database distributed with CTH. In all UAH simulations, the penetrator was also treated with the Mie-Grüneisen EOS (using parameter values for Vascomax-250 steel) and the EPP strength model. The initial yield strength $Y_{01} = 1.16$ GPa was obtained by converting the measured R_c hardness to Brinell (BHN 400) and using a handbook value for oil-quenched and tempered 4130 steel (Brades 1978).

An important factor in the use of CTH is the numerical fracture algorithm. Since strength effects were believed significant in the experiments, we used the maximum principal stress criterion,

$p_f = \max(0, \sigma_{\max}^d - \sigma_f)$, in which σ_f is the smallest (user input) tensile *fracture stress* in the cell, σ_{\max}^d the maximum principal deviatoric stress, and p_f is the cell *fracture pressure*. If the cell pressure falls below p_f , void is introduced to raise the pressure. Use of an experimentally determined spall strength for the fracture stress may not produce good results in all problems; no fracture stress values are supplied in the CTH material libraries. As a baseline value we used $\sigma_f = 1.5 Y_0$ for both materials. The yield strength for mixed cells is given by a volume average over the materials with strength (void volume is not counted). The penetrator-target interface is treated as a contact (continuous velocity). All 3D simulations used a uniform space mesh of 0.075-cm cubes; the mesh and target are longer in the x-direction than indicated in Figure 1.

The Johnson-Cook flow law and failure models (Johnson and Cook 1985) were used for some of the 3D ARL simulations and with the explicit shear band calculations. The flow stress is given by

$$\sigma = [A + B(\epsilon^p)^n] [1 + C \ln(\max(1, \dot{\epsilon}))] [1 - T^{*m}], \quad (1)$$

where ϵ^p is the equivalent plastic strain, $\dot{\epsilon}$ the strain rate and T^* the homologous temperature. The equivalent plastic strain at failure is given by

$$\epsilon^{pf}(p, \sigma, T^*, \dot{\epsilon}) = [D_1 + D_2(-D_3 p/\sigma)] [1 + D_4 \ln(\max(1, \dot{\epsilon}))] [1 + D_5 T^*], \quad (2)$$

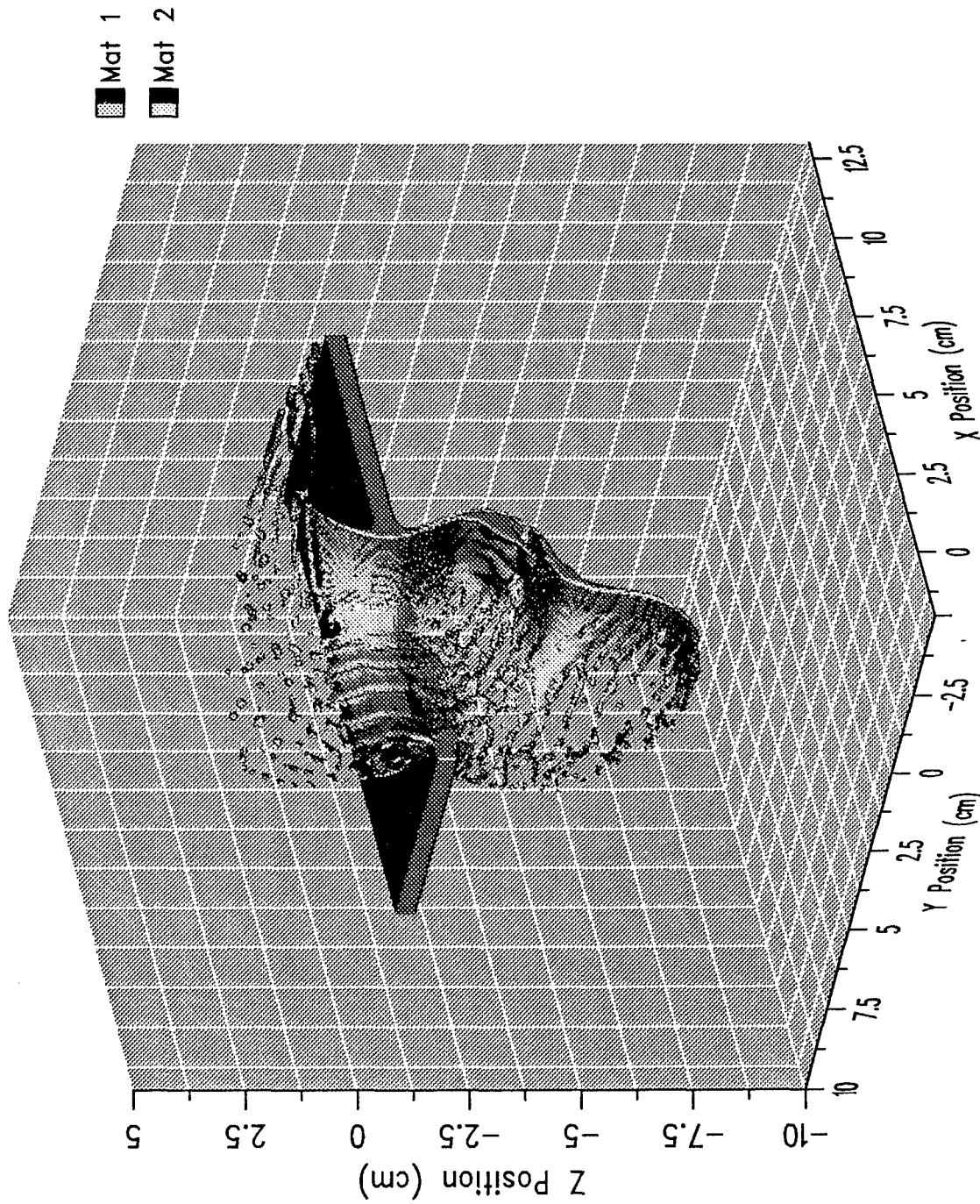
where p is the pressure and D_1, \dots, D_5 are constants. Damage accumulates according to $D = \int (\epsilon^{pf})^{-1} d\epsilon^p$; failure occurs when $D = 1$, at which point (in CTH) the stress deviator and fracture stress, p_f , are set to zero. Material constants were obtained by taking published values for 4340 steel and adjusting A, B, D_1, D_2 so that the yield strength, ultimate strength and ϵ^{pf} in a quasi-static tension test matched handbook values (Brades 1978) for the penetrator.

4. Results of Simulations

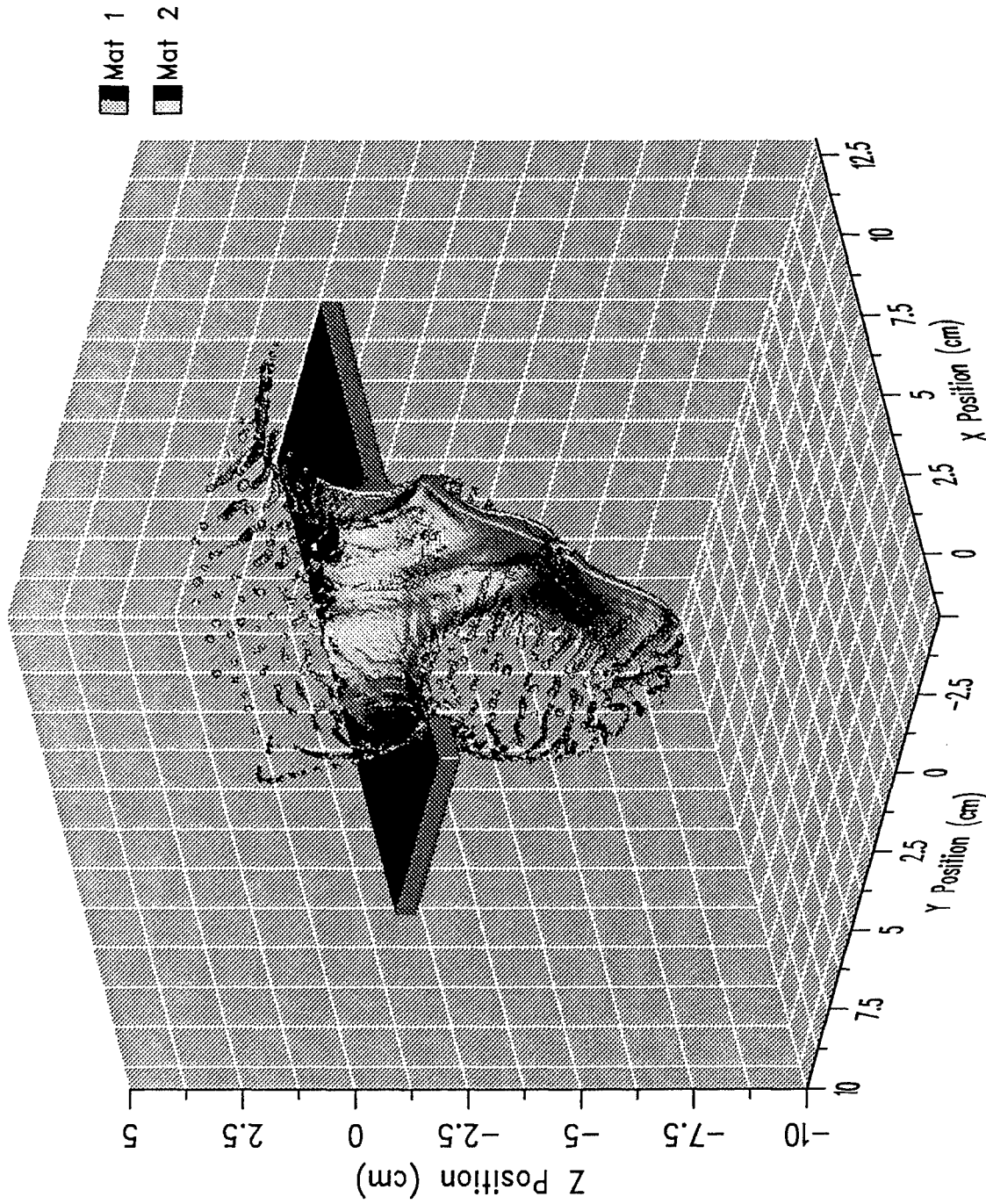
The UAH results are typified by Figure 2. The flow is pressure-dominated and results in considerable fragmentation, although large sections of the debris bubble are still intact. The rotation, ϕ , has a mild effect on the bubble at $\theta = 55^\circ$ but a much stronger effect at 70° . In both cases the edge strike produces a considerably stronger initial shock, which contributes to debris bubble asymmetry. Although little penetrator mass has traveled downrange at 70° , the plate is perforated nonetheless; in all cases, the target hole is still growing at 26 μ s. At 65° and 70° , a large section of plate has been accelerated and deformed by the penetrator, but it is unclear whether these areas will ultimately fragment, tear off as intact petals, or remain attached. Shearing-induced flow instabilities appear to influence the fragmentation significantly, but mesh size dependence of this aspect of the simulations has not yet been explored. Note that although initial shock pressures at $\theta = 55^\circ$ approach 50 GPa (not shown) the impact geometry results in poor focusing of release waves, so there is essentially no shatter of the penetrator. Apparently for the same reason, the well-known α - ϵ phase transition at 13 GPa has no significant effect. By using the CTHED post-processor to sum material masses over subregions of the computational domain, the uprange/downrange partitioning of penetrator mass and target hole growth can be calculated as in Figures 3 and 4.

Figure 5 shows the effect of varying the material failure model at 1.5 km/s. The penetrator fragments in all cases, but only after suffering very extensive plastic deformation, contrary to the experimental results of Bjerke, Luther, and Scheffler (1994). Tensile stresses occur because the penetrator material is flowing laterally against the target. The Johnson-Cook model does not encourage fragmentation, because plastic strain must be accompanied by significant tension in order that damage may accumulate rapidly. During early shock release wave interaction, there is little plastic strain and at later times (as in this figure) the tensile stresses are weak.

To obtain better fragmentation behavior, we have also employed in two dimensions a model intended to capture effects of *adiabatic shear band* formation (Silling 1992). In our version, shear bands are assumed to nucleate (at preassigned locations identified by *Lagrangian tracer particles*)



(a)
Figure 2. Combined Effects of Obliquity, θ , and Rotation, ϕ , on Debris Cloud Evolution at 4.1 km/s and 26 μ s; Impact Velocity Vector Lies in x-z Plane. Plot Volumes Are $9 \times 9 \times 9$ cm, Centered at $(x, y, z) = (4.5, 4.5, -2.5)$. ID = q: $V = 4.16$ km/s, $\theta = 55^\circ$, $\phi = 0^\circ$.



(b)

Figure 2. Combined Effects of Obliquity, θ , and Rotation, ϕ , on Debris Cloud Evolution at 4.1 km/s and 26 μ s; Impact Velocity Vector Lies in x-z Plane. Plot Volumes Are $9 \times 9 \times 9$ cm, Centered at $(x, y, z) = (4.5, 4.5, -2.5)$. ID = w: $V = 4.16$ km/s, $\theta = 55^\circ$, $\phi = 45^\circ$ (continued).

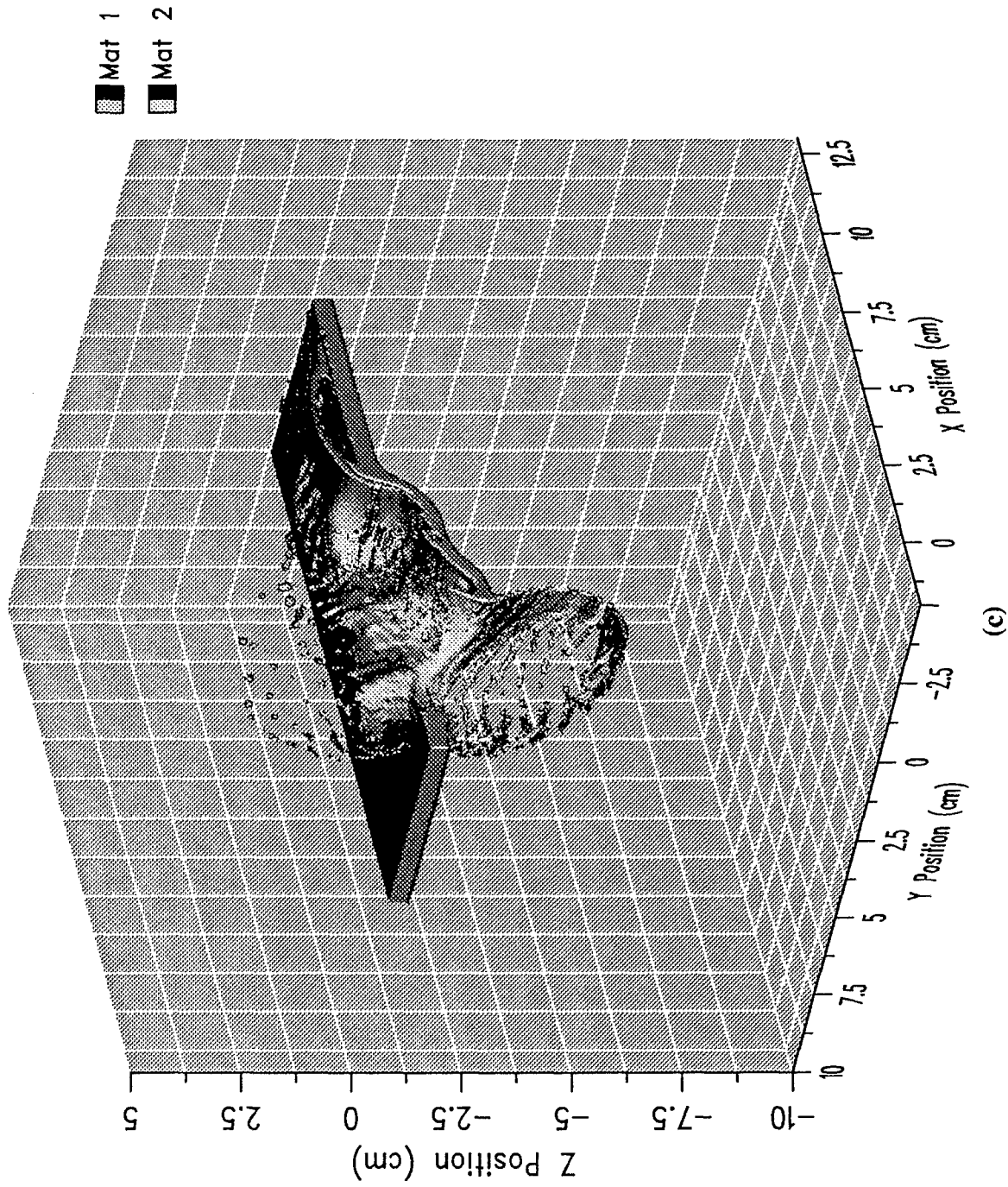


Figure 2. Combined Effects of Obliquity, θ , and Rotation, ϕ , on Debris Cloud Evolution at 4.1 km/s and 26 μ s; Impact Velocity Vector Lies in x-z Plane. Plot Volumes Are $9 \times 9 \times 9$ cm, Centered at $(x, y, z) = (4.5, 4.5, -2.5)$. ID = m: $V = 4.16$ km/s, $\theta = 70^\circ$, $\phi = 0^\circ$ (continued).

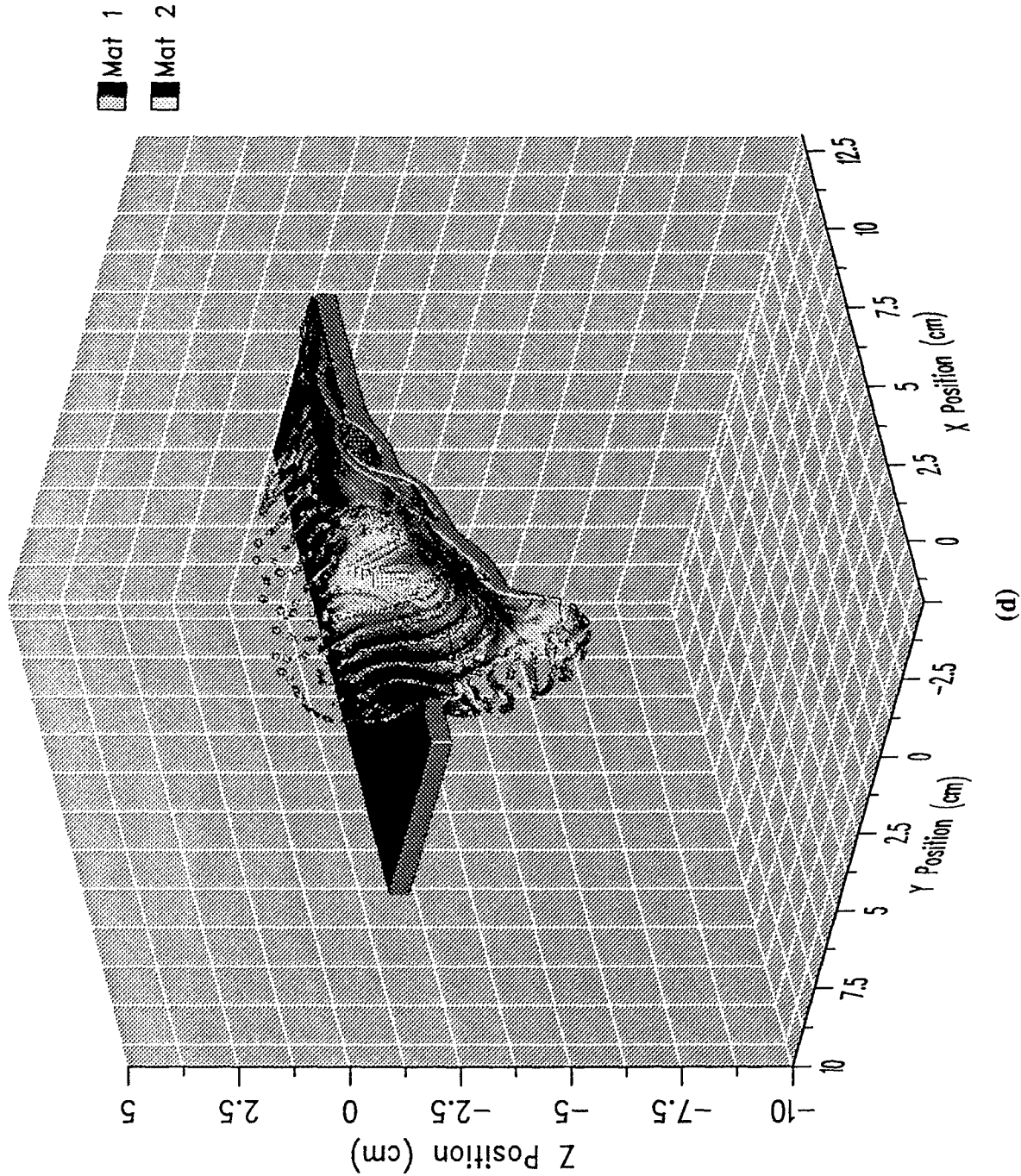


Figure 2. Combined Effects of Obliquity, θ , and Rotation, ϕ , on Debris Cloud Evolution at 4.1 km/s and 26 μ s; Impact Velocity Vector Lies in x-z Plane. Plot Volumes Are $9 \times 9 \times 9$ cm, Centered at $(x, y, z) = (4.5, 4.5, -2.5)$. ID = k: $V = 4.16$ km/s, $\theta = 70^\circ$, $\phi = 45^\circ$ (continued).

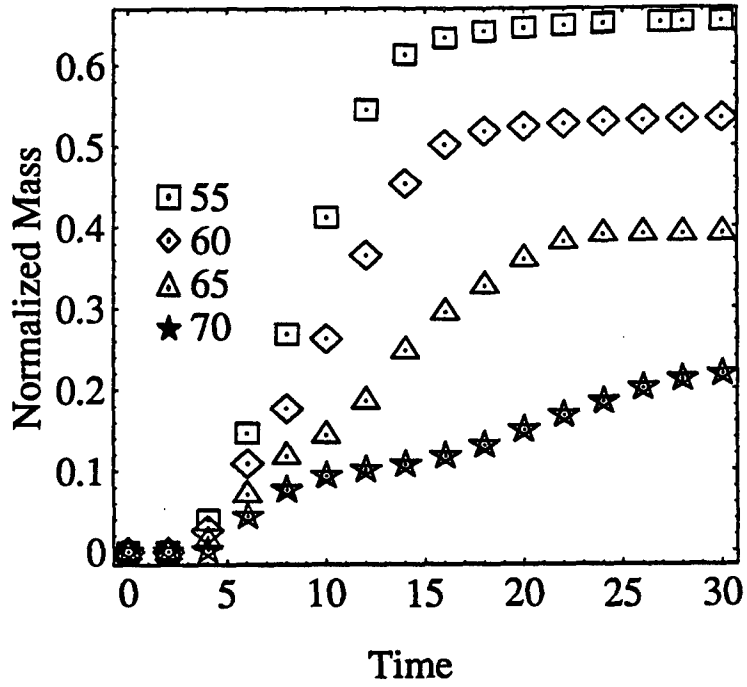


Figure 3. Time History of the Penetrator Mass Fraction Exiting the Bottom of the Target at 4.1 km/s.

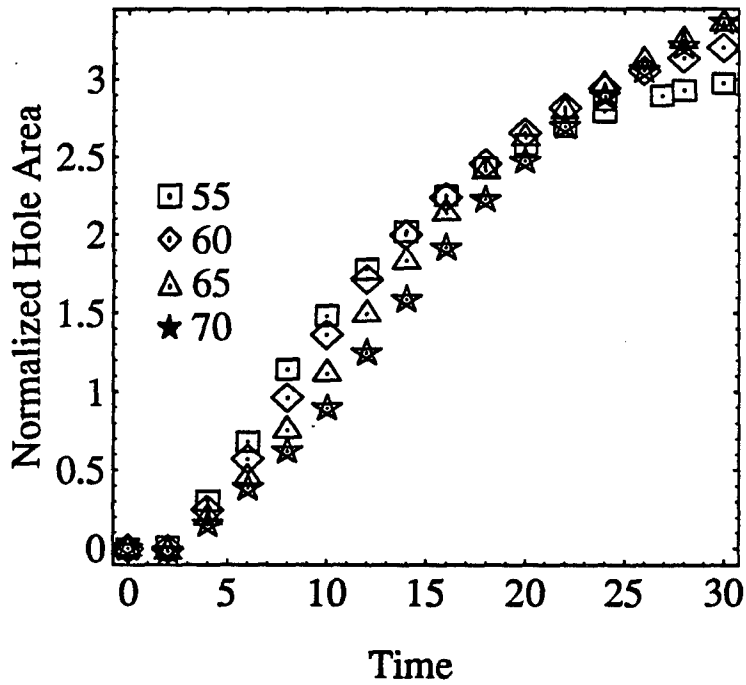


Figure 4. Time History of Target Hole Area Normalized by Sphere-Equivalent Penetrator Area at 4.1 km/s.

when the equivalent plastic strain, ϵ^p , reaches an assigned value, ϵ_{init} . Each nucleator spawns four shear band tips that propagate at speed v_g in the directions of maximum shear stress if ϵ^p exceeds another value $\epsilon_{prop} < \epsilon_{init}$ in the CTH cell containing the band tip. When the tip moves to a new cell, a tracer is inserted and the stress deviator set to zero. On the time scale of our simulations, shear bands are hot and thus weak in tension as well as shear. To account for this, we use (2) with $D_1 = 1$ and $D_2 = \dots = D_5 = 0$, so that when $\epsilon^p \geq 1$, $p_f = 0$. The results in Figure 6 were obtained with $v_g = 2$ km/s, $\epsilon_{init} = 0.3$, $\epsilon_{prop} = 0.05$. In spite of the crude shear band kinetics currently employed, the model does capture a crucial feature of the ARL experiments: the penetrator fractures without the individual fragments having first suffered large plastic deformation. This is particularly evident at the higher obliquities. Among several improvements we intend to make to the physics in this model are:

- a. Directly modify the fracture pressure in shear-banded cells [rather than use equation (2)] to prevent nonphysical softening in unbanded cells.
- b. Allow partial rather than total loss of shear strength in banded cells using results from one-dimensional (1D) analyses of adiabatic shear bands (Walter 1992; Wright 1995) .
- c. Allow random band nucleation with spacing determined from 1D analyses (Wright 1995).

5. Discussion

This work is part of an ongoing effort within the Weapons and Materials Research Directorate to provide improved analytical modeling of high-obliquity impacts. In achieving this end, direct simulation with wavecodes is a critical adjunct to experimentation, provided the simulations include appropriate models for operative material flow and failure mechanisms. In order to maximize the utility of these simulations, one further capability that is required is a statistical description of the debris evolution. This sort of information has traditionally not been available from wavecodes and the current version of CTH is no exception. At present, the CTHED post-processor can sum mass

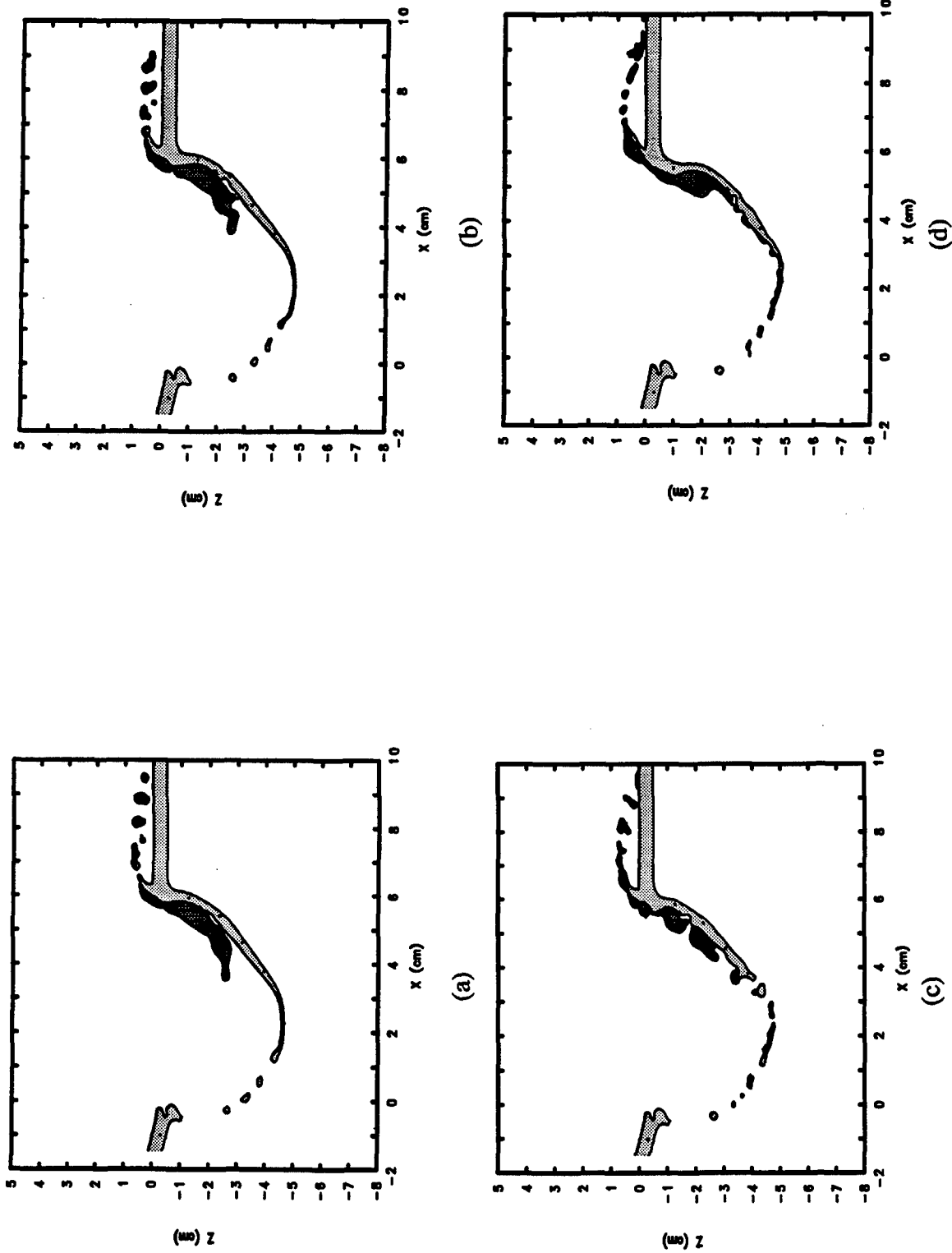
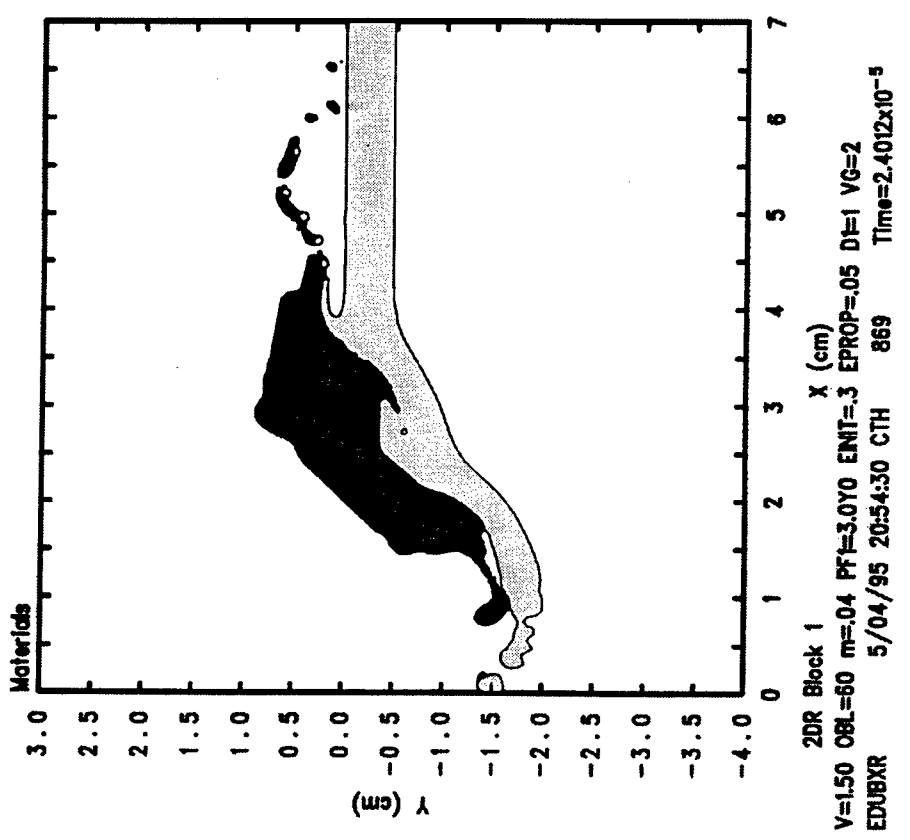
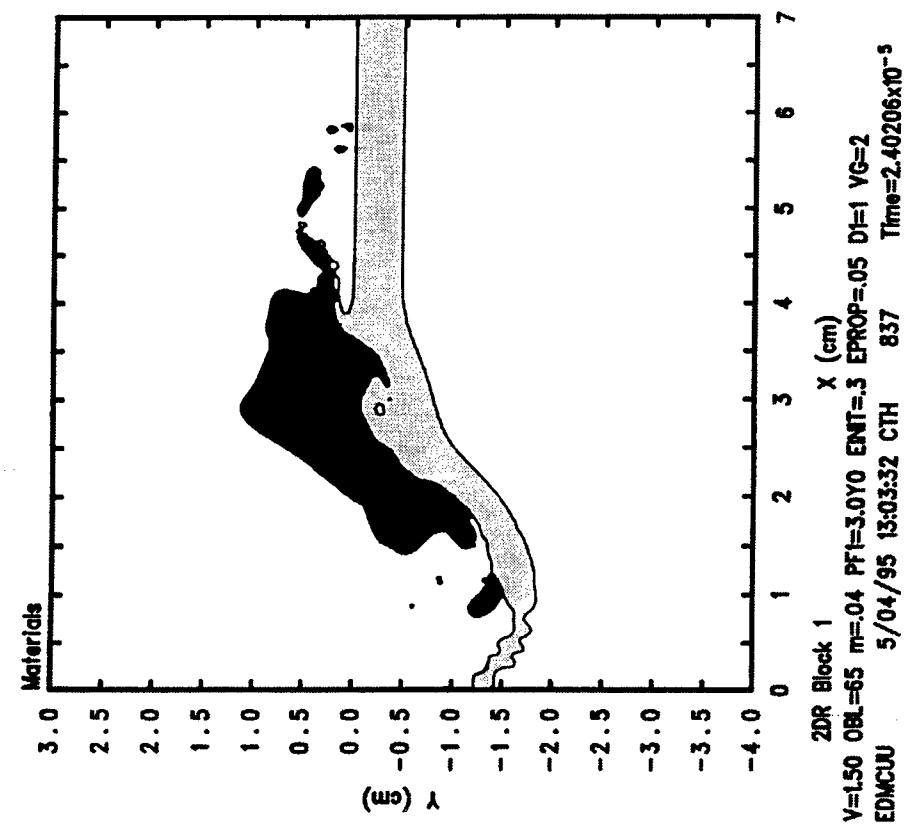


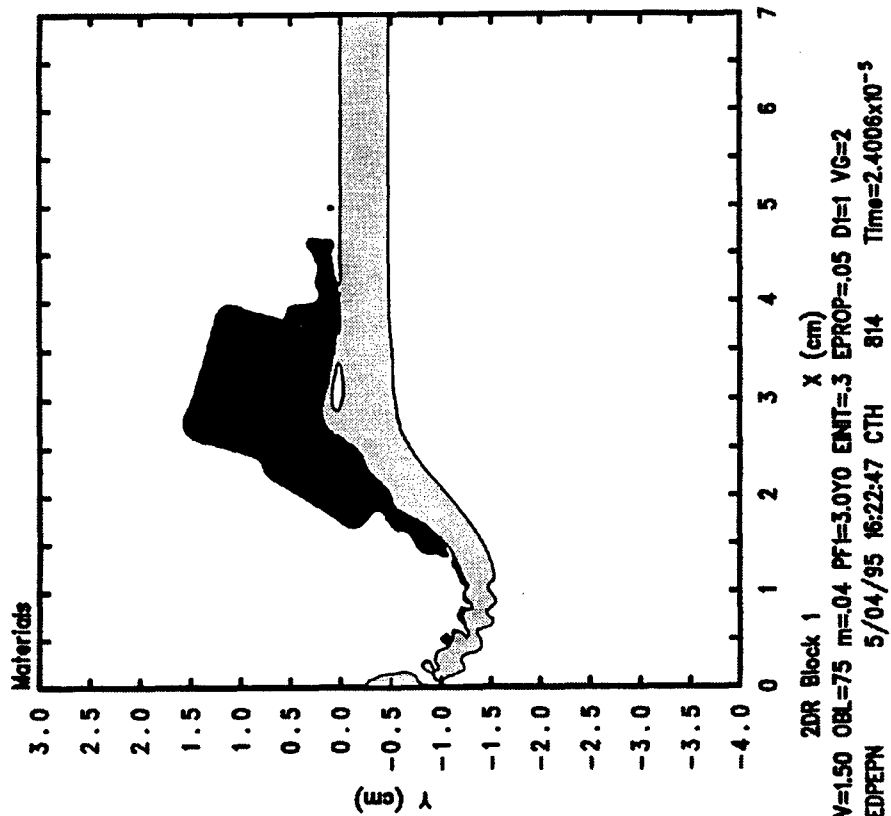
Figure 5. Central Section ($y = 0$) Plots at 1.5 km/s, 60 μ s, and 60° Obliquity Showing Effect of Penetrator Material Failure Model on Fragmentation. (See Table 2 for Parameter Values.) Tensile Fracture Stress, σ_B , in (c) Is 1/4 That in (a), Johnson-Cook Failure Strain, ϵ^{pf} , in (d) Is 1/4 That in (b). Baseline Target Material Parameters Are Used in All Cases.



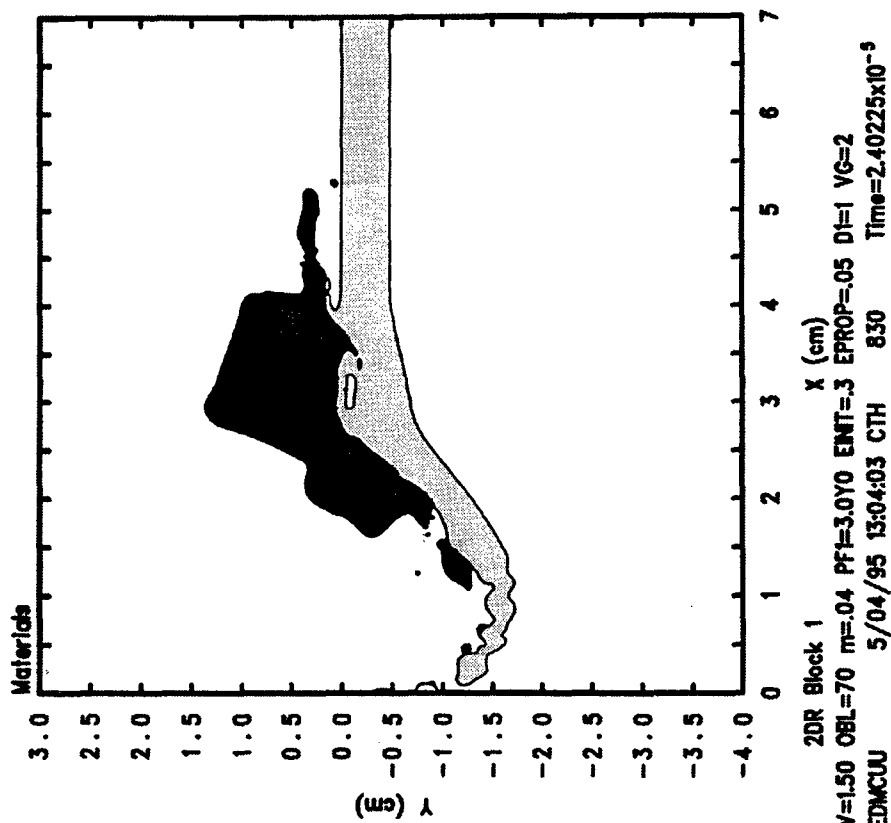
(a)

(b)

Figure 6. Behavior of the Two-Dimensional (2D) Explicit Shear Band Model at 1.5 km/s and 24 μ s. The Black Curves Running Through the Darker Penetrator Material Are the Shear Bands. The Bands Nucleated From Three Tracers Along the Short Edge and Five Along the Long Edge Meeting at the Penetrator Vertex That First Impacted the Target. (a) Obliquity = 60°; (b) Obliquity = 65°.



(c)



(d)

Figure 6. Behavior of the Two-Dimensional (2D) Explicit Shear Band Model at 1.5 km/s and 24 μ s. The Black Curves Running Through the Darker Penetrator Material Are the Shear Bands. The Bands Nucleated From Three Tracers Along the Short Edge and Five Along the Long Edge Meeting at the Penetrator Vertex That First Impacted the Target. (c) Obliquity = 70°; (d) Obliquity = 75° (continued).

over rectangular subregions of the mesh, but more detailed information is not available. More fundamentally, the fragment size produced by the numerical fracture algorithm is generally dependent on the size of the computational cells, although the overall distributions of mass, energy, etc., are less strongly affected by the mesh.

In conclusion, we have presented results that indicate a significant effect of penetrator shape on the debris cloud at high velocity and obliquity. At lower velocity, we have shown that a crude adiabatic shear band model can account for experimentally observed penetrator splitting and that simpler failure models do not.

6. References

- Bjerke, T. W., L. A. Luther, and D. R. Scheffler. "Single Fragment Impact With Laminate Targets." ARL-MR-132, U.S. Army Research Laboratory, Aberdeen Proving Ground, MD, 1994.
- Brades, B. P. (ed.). *Metals Handbook: 9th edition*. Vol. 1, p. 422, 1978.
- Finnegan, S. A., L. F. Dimaranan, O. E. R. Heimdahl, and J. K. Pringle. "A Study of Obliquity Effects on Perforation and Ricochet Processes in Thin Plates Impacted by Compact Penetrators." *Proceedings of the 14th International Symposium on Ballistics*, Quebec Canada, 1993.
- Finnegan, S. A., and J. C. Schulz. "Fragmentation Processes for High-Velocity Impacts." *Shock-Wave and High-Strain-Rate Behavior in Materials*. New York: Marcel Dekker, pp. 705-712, edited by M. A. Meyers, L. E. Murr, and K. R. Staudhammer, 1992.
- Johnson, G. R., and W. H. Cook. "Fracture Characteristics of Three Metals Subjected to Various Strains, Strain Rates, Temperatures and Pressures." *Engineering Fracture Mechanics*, vol. 21, pp. 31-48, 1985.
- McGlaun, J. M., and S. L. Thompson. "CTH: A Three-Dimensional Shock Wave Physics Code." *Journal of Impact Engineering*, vol. 10, pp. 351-360, 1990.
- Silling, S. A. "Shear Band Formation and Self-Shaping in Penetrators." SAND92-2692, Sandia National Laboratory, Albuquerque, NM, 1992.
- Walter, J. W. "Numerical Experiments on Adiabatic Shear Band Formation in One Dimension." *International Journal of Plasticity*, vol. 8, pp. 657-693, 1992.
- Wright, T. W. "Scaling Laws for Adiabatic Shear Bands." To appear in the *International Journal of Solids and Structures*, vol. 32, pp. 2745-2750, 1995.

INTENTIONALLY LEFT BLANK.

<u>NO. OF COPIES</u>	<u>ORGANIZATION</u>
2	DEFENSE TECHNICAL INFORMATION CENTER DTIC DDA 8725 JOHN J KINGMAN RD STE 0944 FT BELVOIR VA 22060-6218
1	HQDA DAMO FDQ DENNIS SCHMIDT 400 ARMY PENTAGON WASHINGTON DC 20310-0460
1	DPTY ASSIST SCY FOR R&T SARD TT F MILTON RM 3EA79 THE PENTAGON WASHINGTON DC 20310-0103
1	OSD OUSD(A&T)/ODDDR&E(R) J LUPO THE PENTAGON WASHINGTON DC 20301-7100
1	CECOM SP & TRRSTRL COMMCTN DIV AMSEL RD ST MC M H SOICHER FT MONMOUTH NJ 07703-5203
1	PRIN DPTY FOR TCHNLGY HQ US ARMY MATCOM AMCDCG T M FISETTE 5001 EISENHOWER AVE ALEXANDRIA VA 22333-0001
1	PRIN DPTY FOR ACQUSTN HQS US ARMY MATCOM AMCDCG A D ADAMS 5001 EISENHOWER AVE ALEXANDRIA VA 22333-0001
1	DPTY CG FOR RDE HQS US ARMY MATCOM AMCRD BG BEAUCHAMP 5001 EISENHOWER AVE ALEXANDRIA VA 22333-0001

<u>NO. OF COPIES</u>	<u>ORGANIZATION</u>
1	INST FOR ADVNCD TCHNLGY THE UNIV OF TEXAS AT AUSTIN PO BOX 202797 AUSTIN TX 78720-2797
1	USAASA MOAS AI W PARRON 9325 GUNSTON RD STE N319 FT BELVOIR VA 22060-5582
1	CECOM PM GPS COL S YOUNG FT MONMOUTH NJ 07703
1	GPS JOINT PROG OFC DIR COL J CLAY 2435 VELA WAY STE 1613 LOS ANGELES AFB CA 90245-5500
1	ELECTRONIC SYS DIV DIR CECOM RDEC J NIEMELA FT MONMOUTH NJ 07703
3	DARPA L STOTTS J PENNELLA B KASPAR 3701 N FAIRFAX DR ARLINGTON VA 22203-1714
1	USAF SMC/CED DMA/JPO M ISON 2435 VELA WAY STE 1613 LOS ANGELES AFB CA 90245-5500
1	US MILITARY ACADEMY MATH SCI CTR OF EXCELLENCE DEPT OF MATHEMATICAL SCI MDN A MAJ DON ENGEN THAYER HALL WEST POINT NY 10996-1786
1	DIRECTOR US ARMY RESEARCH LAB AMSRL CS AL TP 2800 POWDER MILL RD ADELPHI MD 20783-1145

**NO. OF
COPIES ORGANIZATION**

- 1 DIRECTOR
US ARMY RESEARCH LAB
AMSRL CS AL TA
2800 POWDER MILL RD
ADELPHI MD 20783-1145

- 3 DIRECTOR
US ARMY RESEARCH LAB
AMSRL CI LL
2800 POWDER MILL RD
ADELPHI MD 20783-1145

ABERDEEN PROVING GROUND

- 4 DIR USARL
AMSRL CI LP (305)

<u>NO. OF COPIES</u>	<u>ORGANIZATION</u>
3	COMMANDER US ARMY ARDEC AMSTA AR FSA E W P DUNN J PEARSON E BAKER PICATINNY ARSENAL NJ 07806-5000
1	COMMANDER USA STRATEGIC DEFNS CMD CSSD H LL T CROWLES HUNTSVILLE AL 35807-3801
2	COMMANDER US ARMY MICOM AMSMI RD ST WF D LOVELACE M SCHEXNAYDER REDSTONE ARSENAL AL 35898-5250
1	MIS DEFNS & SPACE TECH CSSD SD T K H JORDAN PO BOX 1500 HUNTSVILLE AL 34807-3801
4	COMMANDER US ARMY BELVOIR RD&E CTR STRBE NAE B WESTLICH STRBE JMC T HANSHAW STRBE NAN S G BISHOP J WILLIAMS FORT BELVOIR VA 22060-5166
2	COMMANDER US ARMY RSRCH OFFC K IYER J BAILEY PO BOX 12211 RESEARCH TRIANGLE PARK NC 27709-2211
1	NVL RSRCH LABORATORY A E WILLIAMS CODE 6684 4555 OVERLOOK AVE SW WASHINGTON DC 20375

<u>NO. OF COPIES</u>	<u>ORGANIZATION</u>
1	DIRECTOR NAVAL CIVIL ENGRNG LAB J YOUNG CODE L56 PORT HUENEME CA 93043
1	NAVAL AIR WARFARE CTR S A FINNEGAN PO BOX 1018 RIDGECREST CA 93556
3	COMMANDER NAVAL WEAPONS CTR T T YEE CODE 3263 D THOMPSON CODE 3268 W J MCCARTER CODE 6214 CHINA LAKE CA 93555
12	COMMANDER NVL SURFACE WARFARE CTR DAHLGREN DIVISION H CHEN D L DICKINSON CODE G24 C R ELLINGTON C R GARRETT CODE G22 W HOLT CODE G22 R MCKEOWN W MORTON JR J M NELSON M J SILL CODE H11 W J STROTHER A B WARDLAW JR L F WILLIAMS CODE G33 17320 DAHLGREN RD DAHLGREN VA 22448
5	AIR FORCE ARMAMENT LAB AFATL DLJW W COOK M NIXON AFATL DLJR J FOSTER AFATL MNW LT D LOREY R D GUBA EGLIN AFB FL 32542

<u>NO. OF</u> <u>COPIES</u>	<u>ORGANIZATION</u>
13	COMMANDER NVL SURFACE WARFARE CTR D TASKER CODE 9220 W WILSON P C HUANG CODE G402 B A BAUDLER CODE R12 R H MOFFETT CODE R12 R GARRETT CODE R12 T L JUNGLING CODE R32 R DAMINITY CODE U43 J P MATRA P WALTER L MENSI K KIDDY F J ZERILLI 10901 NEW HAMPSHIRE AVE SILVER SPRING MD 20903-5000
1	USAF PHILLIPS LABORATORY PL WSCD FIROOZ ALLAHDAI 3550 ABERDEEN AVE SE KIRTLAND AFB NM 87117-5776
5	WRIGHT LABS MNMW JOEL W HOUSE ARMAMENT DIRECTORATE STE 326 B1 R D HUNT B MILLIGAN B C PATTERSON W H VAUGHT 101 W EGLIN BLVD EGLIN AFB FL 32542-6810
10	DIRECTOR LANL D MANDELL J V REPA MS A133 E J CHAPYAK MS F664 J DIENES MS B214 D SHARP MS B213 L MARGOLIN MS D413 P HOWE MS P915 L SCHWALBE J GROVE MS B220 M GITTINGS MS B220 PO BOX 1663 LOS ALAMOS NM 87545

<u>NO. OF</u> <u>COPIES</u>	<u>ORGANIZATION</u>
5	DIRECTOR LLNL R E TIPTON L35 D BAUM L35 G POMYKAL L178 A HOLT L290 BMDO R M HALL PO BOX 808 LIVERMORE CA 94550
7	DIRECTOR SANDIA NATL LABS E S HERTEL JR MS 0819 A ROBINSON MS 0819 L N KMETYK MS 0819 R BRANNON MS 0820 M KIPP DIV 1533 P YARRINGTON DIV 1533 M FORRESTAL DIV 1551 PO BOX 5800 ALBUQUERQUE NM 87185
3	ENERGETIC MTRLS RSCH CTR/DOE NEW MEXICO INST OF MINING AND TECH D J CHAVEZ L LIBERSKY F SANDSTROM CAMPUS STATION SOCORRO NM 87801
1	MIT LINCOLN LAB ARMY SCIENCE BOARD W M KORNEGAY 244 WOOD ST RM S2 139 LEXINGTON MA 02173
3	BROWN UNIVERSITY DIV OF ENGINEERING R CLIFTON B FREAND A NEEDLEMAGA PROVIDENCE RI 02912

<u>NO. OF COPIES</u>	<u>ORGANIZATION</u>
3	CALTECH T J AHRENS MS 252 21 W KNAUSS MS 105-50 G RAVICHANDRAN MS 105-50 1201 E CALIFORNIA BLVD PASADENA CA 91125
1	GEORGIA INST OF TECH SCHOOL OF MATL SCIENCE AND ENGINEERING K LOGAN ATLANTA GA 30332-0245
2	JOHNS HOPKINS UNIV DEPT OF MECH ENGR LATROBE HALL A DOUGLAS K RAMESH 34TH AND CHARLES ST BALTIMORE MD 21218
2	SOUTHWEST RSRCH INST C ANDERSON J WALKER PO DRAWER 28510 SAN ANTONIO TX 78284
2	UC SAN DIEGO DEPT APPL MECH AND ENG SVCS R011 S NEMAT-NASSER M MEYERS LA JOLLA CA 92093-0411
2	UNIV OF ALA HUNTSVILLE AEROPHYSICS RSCH CTR G HOUGH D J LIQUORNIK PO BOX 999 HUNTSVILLE AL 35899
1	UNIV OF ALA HUNTSVILLE CIVIL ENGRNG DEPT W P SCHONBERG HUNTSVILLE AL 35899

<u>NO. OF COPIES</u>	<u>ORGANIZATION</u>
2	UNIV OF DAYTON RSCH INST KLA14 N BRAR A PIEKUTOWSKI 300 COLLEGE PARK DAYTON OH 45469-0182
2	UNIV OF MARYLAND DEPT OF MECH ENGR R ARMSTRONG J DALLY COLLEGE PARK MD 20742
1	UNIV OF TEXAS DEPT OF MECH ENGR E P FAHRENTHOLD AUSTIN TX 78712
1	NORTH CAROLINA STATE UNIVERSITY DEPT OF MECH AND AEROSPACE ENGINEERING M ZIKRY RALEIGH NC 27695
1	VIRGINIA POLYTECHNIC INST COLLEGE OF ENGR R BATRA BLACKSBURG VA 24061-0219
3	ALLIANT TECH SYS INC T HOLMQUIST MN11 2720 R STRYK G R JOHNSON MN11 2925 600 SECOND ST NE HOPKINS MN 55343
1	APPLIED RSRCH ASSOC INC J D YATTEAU 5941 S MIDDLEFIELD RD STE 100 LITTLETON CO 80123
2	APPLIED RSRCH ASSOC D GRADY F MAESTAS 4300 SAN MATEO BLVD SE ALBUQUERQUE NM 87110

<u>NO. OF COPIES</u>	<u>ORGANIZATION</u>
1	CALIFORNIA RSCH AND TECH M MAJERUS PO BOX 2229 PRINCETON NJ 08543
1	COMPUTATIONAL MECH CONSULTANTS J A ZUKAS PO BOX 11314 BALTIMORE MD 21239-0314
3	DYNA EAST CORP P C CHOU R CICCARELLI W FLIS 3620 HORIZON DRIVE KING OF PRUSSIA PA 19406
2	GRC INTERNATIONAL T M CUNNINGHAM W M ISBELL 5383 HOLLISTER AVE SANTA BARBARA CA 93111
6	INST OF ADVANCED TECH UNIV OF TX AUSTIN S J BLESS J CAZAMIAS H D FAIR T M KIEHNE D LITTLEFIELD M NORMANDIA 4030 2 W BRAKER LN AUSTIN TX 78759
1	INTERNATIONAL RSRCH ASSOCIATION D ORPHAL 4450 BLACK AVE PLEASANTON CA 94566
1	KAMAN SCIENCES CORP D L JONES 2560 HUNTINGTON AVE STE 200 ALEXANDRIA VA 22303

<u>NO. OF COPIES</u>	<u>ORGANIZATION</u>
8	KAMAN SCIENCES CORP J ELDER R P HENDERSON D A PYLES F R SAVAGE J A SUMMERS J S WILBECK T W MOORE T YEM 600 BLVD S STE 208 HUNTSVILLE AL 35802
3	KAMAN SCIENCES CORP S JONES G L PADEREWSKI R G PONZINI 1500 GRDN OF THE GODS RD COLORADO SPRINGS CO 80907
1	KAMAN SCIENCES CORP N ARI PO BOX 7463 COLORADO SPRINGS CO 80933-7463
1	ORLANDO TECHNOLOGY INC D A MATUSKA PO BOX 855 SHALIMAR FL 32579
1	ROCKWELL INTERNATIONAL ROCKETDYNE DIV H LEIFER 16557 PARK LN CIRCLE LOS ANGELES CA 90049
1	ROCKWELL MISSILE SYS DIV T NEUHART 1800 SATELLITE BLVD DULUTH GA 30136
2	SAIC J FURLONG G J STRUACH 1710 GOODRIDGE DR MCLEAN VA 22102

NO. OF
COPIES ORGANIZATION

NO. OF
COPIES ORGANIZATION

5 SRI INTERNATIONAL
J D COLTON
D CURRAN
R KLOOP
R L SEAMAN
D A SHOCKEY
333 RAVENSWOOD AVE
MENLO PARK CA 94025

1 ZERNOW TECHNICAL
SERVICES INC
L ZERNOW
425 W BONITA AVE STE 208
SAN DIMAS CA 91773

ABERDEEN PROVING GROUND

50 DIR USARL
AMSRL WM I MAY
AMSRL WM MC J WELLS
AMSRL WM MF
T WEERASCORIYA
D DANDEKAR
A RAJENDRAN
AMSRL WM T W F MORRISON
AMSRL WM TA
M BURKINS
W GILLICH
W BRUCHEY
J DEHN
G FILBEY
W A GOOCH
H W MEYER
E J RAPACKI
J RUNYEON
AMSRL WM TB
R FREY
P BAKER
R LOTTERO
J STARKENBERG
AMSRL WM TC
W S DE ROSSET
T W BJERKE
R COATES
F GRACE
K KIMSEY
M LAMPSON
D SCHEFFLER
S SCHRAML
G SILSBY

B SORENSEN
R SUMMERS
W WALTERS
AMSRL WM TD
A M DIETRICH
P KINGMAN (5 CPS)
K FRANK
M RAFTENBERG
M SCHEIDLER
S SCHOENFELD
S SEGLETES
J WALTER (5 CPS)
T WRIGHT
AMSRL WM WD
J POWELL
A PRAKASH

<u>NO. OF COPIES</u>	<u>ORGANIZATION</u>
1	EMBASSY OF AUSTRALIA R WOODWARD COUNSELLOR DEFENCE SCIENCE 1601 MASSACHUSETTS AVE NW WASHINGTON DC 20036-2273
1	CANADIAN ARSENALS LTD P PELLETIER 5 MONTEE DES ARSENAUX VILLIE DE GRADEUR PQ J5Z2 CANADA
1	DEFENCE RSRCH ESTAB SUFFIELD D MACKAY RALSTON ALBERTA TOJ 2NO RALSTON CANADA
1	DEFENCE RSRCH ESTAB SUFFIELD C WEICKERT BOX 4000 MEDICINE HAT ALBERTA T1A 8K6 CANADA
1	DEUTSCHE AEROSPACE AG M HELD POSTFACH 13 40 D 86523 SCHROBENHAUSEN GERMANY
1	DIEHL GBMH AND CO M SCHILDKNECHT FISCHBACHSTRASSE 16 D 90552 RÖT BENBACH AD PEGNITZ GERMANY
5	ERNST MACH INST V HOHLER E SCHMOLINSKE E SCHNEIDER A STILP K THOMA ECKERSTRASSE 4 D 7800 FREIBURG I BR 791 4 GERMANY

<u>NO. OF COPIES</u>	<u>ORGANIZATION</u>
3	FRAUNHOFER INSTITUT FUER KURZZEITDYNAMIK ERNST MACH INSTITUT H ROTHENHAEUSLER H SENF E STRASSBURGER HAUPTSTRASSE 18 D79576 WEIL AM RHEIN GERMANY
5	RAFAEL BALLISTICS CNTR E DEKEL Y PARTOM G ROSENBERG Z ROSENBERG Y YESHURUN PO BOX 2250 HAIFA 31021 ISRAEL
1	TECHNION INST OF TECH FACULTY OF MECH ENG S BODNER TECHNION CITY HAIFA 32000 ISRAEL
4	HIGH ENERGY DENSITY RSRCH V E FORTOV G I KANEL V A SKVORTSOV O YU VOJOBIEV IZHORSKAJA STR 13/19 MOSCOW 127412 RUSSIAN REPUBLIC
2	LAVRENTYEV INST HYDRODYNAMICS L A MERZHIEVSKY V V SILVESTROV NOVOSIBIRSK 630090 RUSSIAN REPUBLIC

<u>NO. OF COPIES</u>	<u>ORGANIZATION</u>
6	DEFENCE RESEARCH AGENCY W A J CARSON I CROUCH C FREW T HAWKINS B JAMES B SHRUBSALL CHOBHAM LANE CHERTSEY SURREY KT16 OEE UNITED KINGDOM
1	ROYAL ARMAMENT R&D ESTAB I CULLIS FORT HALSTEAD SEVEN OAKS KENT TN14 7BJ UNITED KINGDOM
1	UK MINISTRY OF DEFENCE G J CAMBRAY CBDE PORTON DOWN SALISBURY WILTSHIRE SPR OJQ UNITED KINGDOM
2	UNIVERSITY OF KENT UNIT FOR SPACE SCIENCES P GENTA P RATCLIFF CANTERBURY KENT CT2 7NR UNITED KINGDOM
7	INSTITUTE FOR PROBLEMS IN MATERIALS STRENGTH S FIRSTOV B GALANOV O GRIGORIEV V KARTUZOV V KOVTUN Y MILMAN V TREFILOV 3, KRHYZHANOVSKY STR 252142, KIEV-142 UKRAINE
1	INSTITUTE FOR PROBLEMS OF STRENGTH G STEPANOV TIMIRYAZEVSKEY STR 2 252014 KIEV UKRAINE

INTENTIONALLY LEFT BLANK.

REPORT DOCUMENTATION PAGE

Form Approved
OMB No. 0704-0188

Public reporting burden for this collection of information is estimated to average 1 hour per response, including the time for reviewing instructions, searching existing data sources, gathering and maintaining the data needed, and completing and reviewing the collection of information. Send comments regarding this burden estimate or any other aspect of this collection of information, including suggestions for reducing this burden, to Washington Headquarters Services, Directorate for Information Operations and Reports, 1215 Jefferson Davis Highway, Suite 1204, Arlington, VA 22202-4302, and to the Office of Management and Budget, Paperwork Reduction Project (0704-0188), Washington, DC 20503.

1. AGENCY USE ONLY (Leave blank)

2. REPORT DATE

January 1998

3. REPORT TYPE AND DATES COVERED

Final, October 1994 - October 1995

4. TITLE AND SUBTITLE

High-Obliquity Impact of a Compact Penetrator on a Thin Plate: Penetrator Splitting and Adiabatic Shear

5. FUNDING NUMBERS

62618AH80

6. AUTHOR(S)

J. W. Walter and P. W. Kingman

7. PERFORMING ORGANIZATION NAME(S) AND ADDRESS(ES)

U.S. Army Research Laboratory
ATTN: AMSRL-WM-TD
Aberdeen Proving Ground, MD 21005-5066

8. PERFORMING ORGANIZATION REPORT NUMBER

ARL-TR-1584

9. SPONSORING/MONITORING AGENCY NAMES(S) AND ADDRESS(ES)

10. SPONSORING/MONITORING AGENCY REPORT NUMBER

11. SUPPLEMENTARY NOTES

12a. DISTRIBUTION/AVAILABILITY STATEMENT

Approved for public release; distribution is unlimited.

12b. DISTRIBUTION CODE

13. ABSTRACT (Maximum 200 words)

Computational simulations were performed of the impact of a compact, nonideal penetrator on a thin plate at high obliquities. These computations simulated two series of experiments at velocities of 1.5 km/s and 2.2 km/s, respectively, with obliquities of 55–70°.

The experimental results indicated penetrator splitting at obliquities between 55 and 65°. Preliminary three-dimensional simulations with the CTH code, using either maximum tensile stress failure or the Johnson-Cook model, captured some aspects of fragment splitting but in a less than satisfactory manner. Simulations utilizing the Silling shear band model were also performed, with somewhat more realistic results.

In addition to graphical descriptions of the target hole geometry and debris cloud, numerical histories of the target hole area and up-range/down-range partitioning of mass, momentum, and energy were extracted for comparison with the experiments.

14. SUBJECT TERMS

penetration, high-obliquity debris, adiabatic shear

15. NUMBER OF PAGES

31

16. PRICE CODE

17. SECURITY CLASSIFICATION OF REPORT

UNCLASSIFIED

18. SECURITY CLASSIFICATION OF THIS PAGE

UNCLASSIFIED

19. SECURITY CLASSIFICATION OF ABSTRACT

UNCLASSIFIED

20. LIMITATION OF ABSTRACT

UL

INTENTIONALLY LEFT BLANK.

USER EVALUATION SHEET/CHANGE OF ADDRESS

This Laboratory undertakes a continuing effort to improve the quality of the reports it publishes. Your comments/answers to the items/questions below will aid us in our efforts.

1. ARL Report Number/Author ARL-TR-1584 (Walter) Date of Report January 1998

2. Date Report Received _____

3. Does this report satisfy a need? (Comment on purpose, related project, or other area of interest for which the report will be used.) _____

4. Specifically, how is the report being used? (Information source, design data, procedure, source of ideas, etc.) _____

5. Has the information in this report led to any quantitative savings as far as man-hours or dollars saved, operating costs avoided, or efficiencies achieved, etc? If so, please elaborate. _____

6. General Comments. What do you think should be changed to improve future reports? (Indicate changes to organization, technical content, format, etc.) _____

CURRENT
ADDRESS

Organization

Name

E-mail Name

Street or P.O. Box No.

City, State, Zip Code

7. If indicating a Change of Address or Address Correction, please provide the Current or Correct address above and the Old or Incorrect address below.

OLD
ADDRESS

Organization

Name

Street or P.O. Box No.

City, State, Zip Code

(Remove this sheet, fold as indicated, tape closed, and mail.)
(DO NOT STAPLE)

DEPARTMENT OF THE ARMY

OFFICIAL BUSINESS

BUSINESS REPLY MAIL
FIRST CLASS PERMIT NO 0001,APG,MD

POSTAGE WILL BE PAID BY ADDRESSEE

DIRECTOR
US ARMY RESEARCH LABORATORY
ATTN AMSRL WM TD
ABERDEEN PROVING GROUND MD 21005-5066



NO POSTAGE
NECESSARY
IF MAILED
IN THE
UNITED STATES

